Membranes of polysulfone and hybrid applied in dye separation

Bruna Aline Araújo[a], Edcleide Maria Araújo[b], Sandriely Sonaly Lima Oliveira[b],
Rodholfo da Silva Barbosa Ferreira[b], Keila Machado de Medeiros[c],*,
Carlos Antônio Pereira de Lima[a]

[a]*Sanitary and Environmental Engineering Department, State University of Paraiba, Avenue Baraunas, 351 Bodocongo,
58429-500 Campina Grande, Paraiba, Brazil, Tel. +55 83 3315 3333; emails: brunaaaraujo15@gmail.com (B.A. Araujo),
caplima@uepb.edu.br (C.A.P. de Lima)*
[b]*Materials Engineering Department, Federal University of Campina Grande, Avenue Aprigio Veloso, 882 Bodocongo,
58429-900 Campina Grande, Paraiba, Brazil, Tel. +55 83 2101 1182; emails: edcleide.araujo@ufcg.edu.br (E.M. Araújo),
sandrielysonaly1@gmail.com (S.S.L. Oliveira), rodholfoferreira@gmail.com (R.S.B. Ferreira)*
[c]*Science and Technology Center in Energy and Sustainability, Federal University of Reconcavo da Bahia, Street Godofredo Rebello de
Figueiredo Filho, 697 Sim, 44085-132 Feira de Santana, Bahia, Brazil, Tel. +55 75 3622 9351; email: keilamedeiros@ufrb.edu.br*

ABSTRACT

In this work, polysulfone (PSU) membranes were prepared with 1.0%, 3.0%, and 5.0% by weight of titanium dioxide (TiO_2). The membranes were analyzed by viscosity, X-ray diffraction (XRD), Fourier transform infrared spectroscopy (FTIR), scanning electron microscopy (SEM), water vapor permeation, contact angle (CA), flow measurements (FM), and yield. Through XRD and FTIR, the PSU membranes and their hybrids showed peaks and bands characteristic of PSU and TiO_2 structure. By SEM and viscosity, it was observed that the addition of TiO_2 promoted the formation of agglomerates on its surface, in addition to increasing the viscosities and thickness of these membranes. Through the CA and of water vapor permeation, it was found that the PSU membrane had the higher angle value and the smallest vapor permeation, probably because it presents a smooth filter skin with few pores and low interconnectivity of these with the porous layer. The separation tests indicated a decrease in flow, due to the fouling formed on the membranes surface and a significant reduction of dye in permeate, allowing the treatment of this contaminant. Furthermore, TiO_2 for being a hydrophilic material and for acting as a porogenic agent, facilitated the passage of water, favoring the dye separation by hybrid membranes.

Keywords: Membranes; Hybrids; Phase inversion; Industrial effluent

1. Introduction

The implementation of cleaner technologies and research in water treatment are the ways to minimize the impacts caused to the environment and improvement of water resources and, consequently, economic, and social of a region. A worldwide trend is the development of processes that use inputs with great efficiency, maximize the reuse of process water, minimizing energy expenditure, and the emission of effluents [1].

Common treatment processes include chemical methods, centrifugation, ultracentrifugation, heat treatments, and among others. Each of these processes has serious limitations, whether, in terms of energy, thermal and mechanical treatments, that is, chemical. Processes that have been receiving increasing attention due to their energy efficiency

* Corresponding author.

are the ones that use membranes as an active principle of their operation, this because it is a clean technology, has the simplicity of operation, has wide applicability, in addition to being possible to combine with other processes [2–4].

The membrane separation processes (MSP), consist of a clean technology, which does not require the greater technical capacity of operation, which can be combined with several other processes, which require simple and small equipment. They are considered efficient technologies for the contribution of solutions to several world problems, such as the treatment of residues from industries, sewers, and rain networks, which are released into the environment, in the form of liquids or gases. Because of this, the growth in research involving membrane synthesis and studies is remarkable. Thus, the MSP is disseminated to industrial levels, this is the result of great advances in studies on membranes, improving their performance for better productivity, greater selectivity, and better stability [5–7].

Membranes are filter media that have pores of varying dimensions. These pores are responsible for the properties that make membranes useful in their various applications, to separate particles and to fractionate molecules of different molar masses [8,9].

Phase inversion is the most used method for obtaining microporous polymeric membranes, which are produced by the precipitation of a polymeric solution spread as a thin film or extruded as hollow fiber, and subsequent precipitation in a non-solvent bath. The membrane is formed by destabilizing the solution and precipitating the polymer. This technique allows us a wide morphological variation from small variations made in the parameters used during the process of preparing the membranes [10–12].

Polysulfone (PSU) is an amorphous, hard, rigid, and highly resistant thermoplastic polymer, being, therefore, characterized as a high-performance polymer, whose main chain is composed of basic repeating units containing sulfone, aryl, and ether groups. Although it can be found in aliphatic or aromatic form, aromatic polysulfone, which is characterized by the presence of di-phenyl-sulfone groups linked in its repeating unit, has better properties for the manufacture of membranes. This has a high glass transition temperature, good mechanical resistance, high hardness (which implies greater resistance to localized plastic deformation), and good thermal and oxidative resistance. Given these characteristics, PSU is being used to obtain polymeric membranes with excellent properties [13–15].

PSU membranes have been widely used for wastewater treatment due to their desired properties, such as stability, high mechanical strength, and ease of modification. The alteration of these membranes presents a great opportunity to improve its performance in the area of wastewater treatment. Up-to-date studies on nanomaterials, as well as hydrophilic macromolecules used in modifying ultrafiltration/microfiltration PSU membranes for application in water treatment, have been extensively analyzed. These modified membranes exhibited a remarkable improvement with respect to water permeability, salt rejection, and antifouling characteristics of PSU-modified membranes when compared to pure PSU membranes. Based on studies carried out, it is evident that PSU membranes modified with hydrophilic nanomaterials and macromolecules have unique characteristics that can contribute to the advancement of innovative nanocomposite membranes with improved wastewater treatment capabilities [16].

The preparation of mixed matrix membranes in which inorganic compounds, such as aluminum oxide (Al_2O_3), titanium dioxide (TiO_2), zirconium oxide (ZrO_2), and silicon dioxide (SiO_2) nanoparticles are incorporated into the polymeric membrane structure, has recently attracted wide attention. The purpose of adding the use of these inorganic materials in the manufacture of polymeric membranes is to decrease the scale, increase the permeability, improve the chemical stability and reinforce the rejection of specific chemical species [17].

The addition of organic and inorganic components to the polysulfone membrane solution has become a widely used technique in the preparation of membranes, and the addition of components characterizes composite membranes [18–21]. TiO_2 has suitable chemical resistance, easily tunable morphology, surface properties, and catalytic functionality besides the antifouling properties of TiO_2 nanoparticles have made them applicable in membrane technology [22]. Consequently, TiO_2 nanoparticles can be used for filtration purposes to increase the membrane resistance against fouling by degrading the organic foulants which come into contact with the nanoparticles within the membrane matrix [23].

Polysulfone ultrafiltration membranes added with TiO_2 nanoparticles and multi-walled carbon nanotube (MWCNT) with variable rates of nanoparticles (NP) were manufactured by the phase inversion method. The effects of the proportion of TiO_2/MWCNT nanoparticles were analyzed on the size and morphology of the membrane pores, permeation, incrustation, and rejection of humic acid (HA). The membranes on which the NPs were combined exhibited an ideal balance of performance and synergism in terms of increased flow combined with high HA rejection [24].

Krishnamoorthy and Sagadevan [25] prepared polyethersulfone (PES) asymmetric membranes blended with polyethylene glycol and iron oxide nanoparticles using the phase inversion technique. Membranes were analyzed for their morphology, thermal stability, and membrane characterization. Morphology studies using scanning electron microscopy (SEM) and atomic force microscopy confirmed the increase in the number of pores, pore size in the support layer, and surface roughness in blended membranes, ensuring the chances of enhanced flux. Surface hydrophilicity was increased with the increase in iron oxide concentration in composite membranes. Thermal analysis studies showed the better thermal stability of blended membranes. The pure water flux of prepared composite membranes was improved to a maximum of four times in comparison with pure PES membrane. Dye rejection studies clearly showed that the blended membranes almost had the same rejection as that of pure PES membranes. Thus, the prepared PES composite UF membrane is a promising candidate for the treatment of dye polluted wastewater, ensuring high fluxes, and effective rejection.

The addition of TiO_2 to the polysulfone membranes provides significant changes in the morphological structure with an increase in the quantity and size of the pores, present on the upper surface of these hybrid membranes.

In addition, it promotes an improved flow, favoring its application in microfiltration systems for the treatment of liquid effluents [26–30]. This work aims to develop microporous flat membranes of polysulfone/titanium dioxide hybrid systems through the phase inversion technique, aiming at its application in the treatment of dye.

2. Experimental

2.1. Materials

For this research, the following materials were used: the polymer matrix used was the polysulfone UDEL P3500 LCD MB7, Fig. 1a, manufactured by Solvay, with a molar mass between 77,000 and 83,000 g mol^{-1} and a relative density of 1.2, according to ASTM D792. O titanium dioxide (TiO$_2$), P-25, identified as Aeroxide® with a purity level of 99.5% in the form of fine powder supplied by Evonik Degussa (Brazil), which consists of 70% of the anatase phase and 30% of the rutile phase. The solvent *n*-methyl 2-pyrrolidone (NMP), Fig. 1b, with 99.5% purity, from the company Synth, was used as a solvent to dissolve the polysulfone and its hybrids to obtain the membranes, with the molecular structure shown in Fig. 1b. The glycerin (C$_3$H$_5$(OH)$_3$) used was with a purity level of 99.5%, molar mass 92.09 g mol^{-1}, acquired by Vetec Fine Chemicals Ltda., (Brazil).

2.2. Preparation of polymeric and hybrid membranes

Initially, the polysulfone, containing TiO$_2$ (1%, 3%, and 5% by weight), were dissolved in the NMP solvent and the solution was stirred for 24 h. Then, the prepared solution was placed on a glass plate, and spread with a glass stick under the plate. The plate was immediately immersed in a bath containing non-solvent, in this case, distilled water. The membranes remained in the bath until their precipitation was completed. Soon after, they were removed from the plates, washed with distilled water, and later, they were dipped in a mixture of 20% w/w glycerin. The membranes were stored in a solution with glycerine to prevent pore collapse, and before being subjected to the permeability test, they were washed with distilled water to eliminate the glycerine. The membranes used to perform the flow measurement test remain submerged in this mixture until the test is performed. The compositions of the systems are shown in Table 1.

2.3. Characterizations of polymeric and hybrid membranes

The viscosities of polymeric and hybrid solutions were analyzed at room temperature, at a speed of 20 rpm, in the microprocessed rotary viscosimeter, manufactured by Quimis Scientific Apparatus Ltda., (Brazil). The polymeric and hybrid membranes were characterized by X-ray diffraction (XRD), using a Shimadzu XRD 6000 equipment (Tokyo, Japan), with λ = 1.541 Å, operating at 40 kV and 30 mA and scanning angle from 1.5° to 30°. The analysis of Fourier transform infrared spectroscopy (FTIR) was performed on a Perkin-Elmer Spectrum 400 spectrometer (Massachusetts, United States) with a scan from 4,000 to 650 cm^{-1}. The images from SEM were obtained in SSX 550 Superscan – Shimadzu equipmen (Tokyo, Japan) t. For analysis of the cross-section, the samples were fractured in liquid nitrogen to prevent plastic deformation. The membranes were coated with gold. The contact angle analysis was performed using the sessile drop method, using a portable contact angle, Phoenix-i model from Surface Electro Optics – SEO. The drop was formed manually by means of a micrometric doser, the image of the drop was captured by the camera embedded in the equipment, where it was later analyzed in the software. All membranes were characterized in the form of thin films.

2.4. Water vapor permeation

This test was carried out according to ASTM E96 [31], using the gravimetric method. The permeability of the films was calculated according to Eq. (1). Where P is the permeability of the films in Barrer, G is the mass that passes through the film per unit area and time that was determined by calculating the slope of the straight line of mass loss of the pots per unit area as a function of time, h is the film thickness, V_0 is 22.414 cm^3 mol^{-1} which is the normal molar volume under standard conditions of temperature and pressure (0°C, 1 atm) of the water vapor, M is 18.011 g mol^{-1} which is the molar mass of the water, P_v is the vapor pressure of the water at the temperature of the experiment and Δu is the relative humidity difference between the interior of the container and the outside.

$$P = \frac{G \cdot h \cdot V_0}{M \cdot P_v \cdot \Delta u} \tag{1}$$

2.5. Water permeability and dye retention

For the flux test measurements with water and water/dye, a perpendicular filtration cell with an effective area of approximately 13.0 cm^2 was used, as shown in Fig. 2, coupled to a filtration system, which was used to measure the permeate.

The membranes were subjected to pressure permeability tests of 1.0 bar and a temperature of 25°C. At least three measurements, for each pressure, were taken to obtain the mean values of the water permeate flux. The permeate samples were collected over a period of 60 min
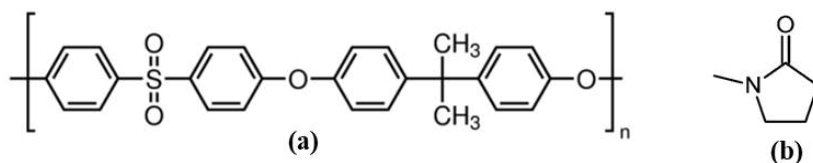
Fig. 1. Molecular structure: (a) polysulfone and (b) *n*-methyl 2-pyrrolidone.

Table 1
Composition of membranes used in this study

Membranes	NMP (%)	Polysulfone (%)	TiO$_2$ (%)
Pure PSU	90	10.0	–
PSU/1% w/w TiO$_2$	90	9.9	0.1
PSU/3% w/w TiO$_2$	90	9.7	0.3
PSU/5% w/w TiO$_2$	90	9.5	0.5
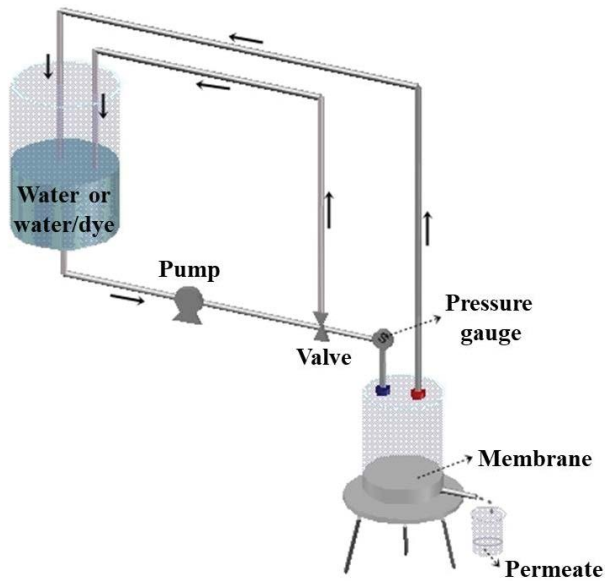
Fig. 2. Filtration system used to estimate the permeate flow with water or water/dye.

for each membrane. The operation was performed at room temperature. The membrane performance was evaluated by permeate flow and selectivity with the indigo blue dye present in the feed solution at a concentration of 200 mg L^{-1}.

The performance of the membranes can be assessed through the permeate flow and the selectivity of a particular solute present in the feed solution. The volumetric flow (J) of the membranes determined by Eq. (2) [32]:

$$J = \frac{\text{Permeate volume (L)}}{\text{Membrane area (m}^2\text{)} \times \text{Time (h)}} \quad (2)$$

From the obtained results, it was possible to draw real profiles of flow measurements, testing the efficiency of these membranes in dye separation. The selectivity of membranes was estimated by rejection coefficient (R%), calculated based on the ratio of concentrations of dye in permeate (C_P) and the feed solution (C_0) expressed by Eq. (3) [32]:

$$R\left(\%\right) = \left[\frac{\left(C_0 - C_P\right)}{C_0}\right] \times 100 \quad (3)$$

The analysis of indigo blue concentrations present in permeate samples was measured using the Bel Photonics spectrophotometer of ultraviolet-visible (UV-vis), model UV-M51, with the concentration of 500 mg L^{-1}. The sample containing indigo blue was transferred to the spectrophotometer cell for reading between 400 and 1,000 nm and the concentration of indigo blue present in the sample was calculated, taking as a basis, the absorbance value measured in equipment. The analysis was performed at the Environmental Science Research Laboratory of the Department of Sanitary and Environmental Engineering of Paraiba State University.

3. Results and discussion

3.1. Viscosity

Fig. 3 illustrates the viscosities of solutions used in the preparation of pure PSU membrane and their hybrids with 1, 3, 5% w/w of TiO$_2$.

The addition of inorganic components to polymeric membrane solution has become a widely used technique in the preparation of membranes, and the addition of components characterizes composite membranes. The viscosity of suspensions is determined by static viscosity measurement as a function of shear rate. The solutions used to obtain the membranes containing 1%, 3%, and 5% by weight of TiO$_2$ showed viscosities of about 2,230; 2,790; and 3,070 mPa s, respectively, these results were higher when compared to the pure PSU membrane with the viscosity of 2,174 mPa s, and this increase was directly proportional to the increase in the percentage of inorganic nanoparticles. In addition, in particular, the viscosity increases significantly, to 3 and 5% w/w of TiO$_2$ content, this fact can be explained due the high specific surface area of TiO$_2$ results in a high surface available for the adsorption of the polysulfone chains. This adsorption of polysulfone in the hydroxyl groups present in the TiO$_2$ spheres causes the formation of a suspension with a mechanically stable structure resulting in a very high viscosity with a low shear rate of 20 rpm. Similar results were obtained by researchers who studied the increase in the percentage of TiO$_2$ nanoparticles in PSU membranes, noting that there were changes in their rheological properties, increasing the solution viscosity [20,21,27–30,33].

3.2. X-ray diffraction

Fig. 4 illustrates the results from XRD of pure PSU membrane and their hybrids with 1, 3, 5% w/w of TiO$_2$.

Polysulfone is an amorphous polymer and in glassy state, it is widely used as a barrier material in separation membranes. According to the diffractogram illustrated in Fig. 4, it was possible to observe a characteristic peak between 15° and 20°, around 17° related to its structure [34]. In general, the hybrid membranes showed the same behavior with a characteristic peak of polysulfone structure and practically the absence of characteristic bands of TiO$_2$, due to an efficient mixture of TiO$_2$ with the polymeric matrix. Furthermore, in hybrid membranes two very discrete peaks of diffraction were visualized at 25.4° and 27.5°, due to the crystalline phase of TiO$_2$, in this case, anatase and rutile, respectively [35].
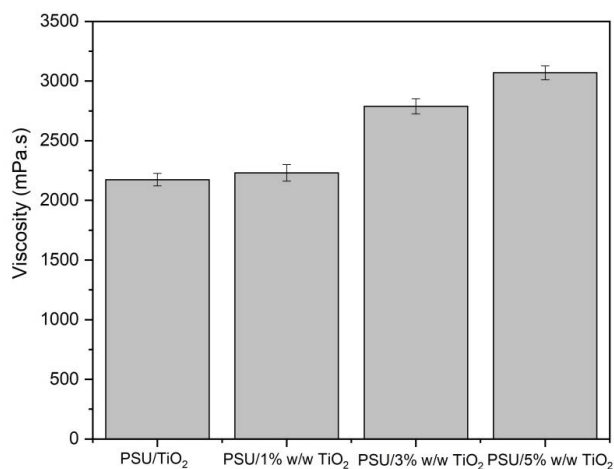
Fig. 3. Viscosities of solutions used in the preparation of pure PSU membrane and hybrids with 1, 3, and 5% w/w TiO$_2$.
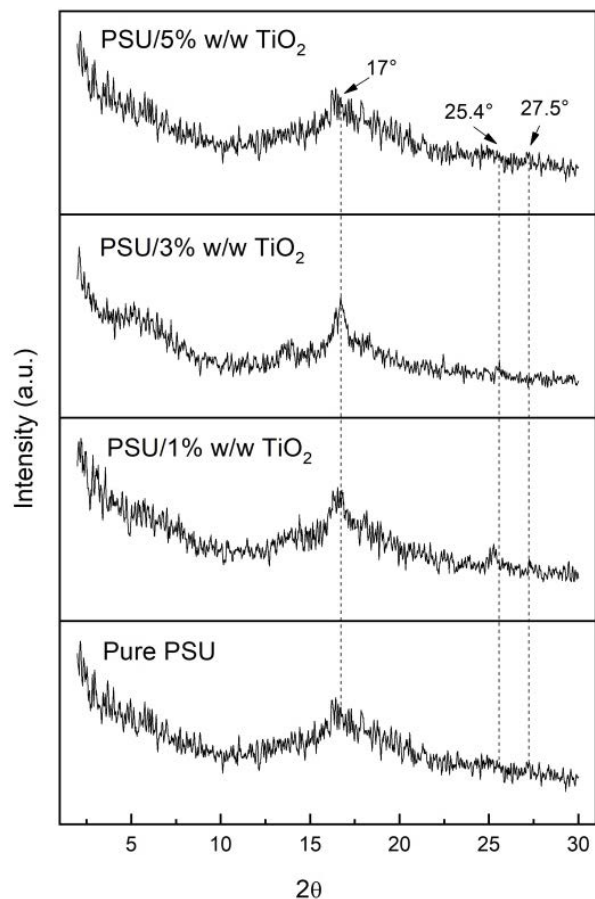
Fig. 4. X-ray diffractograms of pure PSU membrane and hybrids with 1, 3, and 5% w/w TiO$_2$.

3.3. Fourier transform infrared spectroscopy

Fig. 5 shows FTIR analyzes of pure PSU membrane and their hybrids with 1, 3, 5% w/w TiO$_2$. According to the spectra shown in Fig. 5, it was possible to visualize that the characteristic bands of the polymer are: in 1,153 cm^{-1},
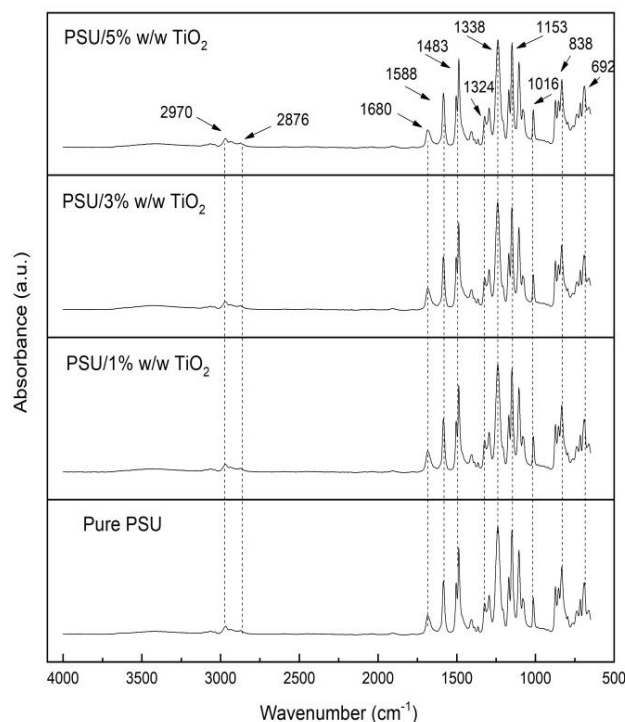
Fig. 5. FTIR spectra of pure PSU membrane and hybrids with 1, 3, and 5% w/w TiO$_2$.

referring to the symmetrical stretching of sulfone; in 1,338 cm^{-1}, of aromatic ether; in 1,324 cm^{-1}, the asymmetric stretching of sulfone; in 2,970 cm^{-1}, of the aromatic stretch of CH$_3$; in 2,876 cm^{-1}, referring the CH$_3$ aliphatic stretch, in 1,483 and 1,588 cm^{-1}, referring to C–C stretch of aromatics; in 1,016 cm^{-1}, referring the asymmetric C–O stretch and in 692 cm^{-1} and, in 838 cm^{-1}, referring the rocking molecular vibration of C–H bond [36–44].

It is also possible to verify in Fig. 5, that the same bands refer to the pure polysulfone membrane and appear in membranes of their hybrids. However, these bands below 1,000 cm^{-1} are not only related to polysulfone but are also inherent the typical characteristic bands of titanium dioxide, related to the vibration of Ti–O and Ti–O–O bonds of TiO$_2$ anatase phase octahedrons that share faces of the TiO$_2$ structural network [45]. They remained superimposed in the polysulfone bands because they had the same wavenumber ranges.

3.4. Scanning electron microscopy

The SEM photomicrographs of the top surface and the cross-section of pure PSU membrane and their hybrids with 1, 3, and 5% w/w TiO$_2$ are shown in Fig. 6. The images were obtained with a fixed increase in the surface of the top of 10,000 times, while in cross-section there were increase variations between 1,400 and 3,000 times.

From Fig. 6, it was possible to observe that the membranes presented an integral anisotropic morphology that can be attributed to the preparation method by phase inversion and by the action of TiO$_2$ (in the case of hybrid membranes). In this method, there is a diffusive mass flow,
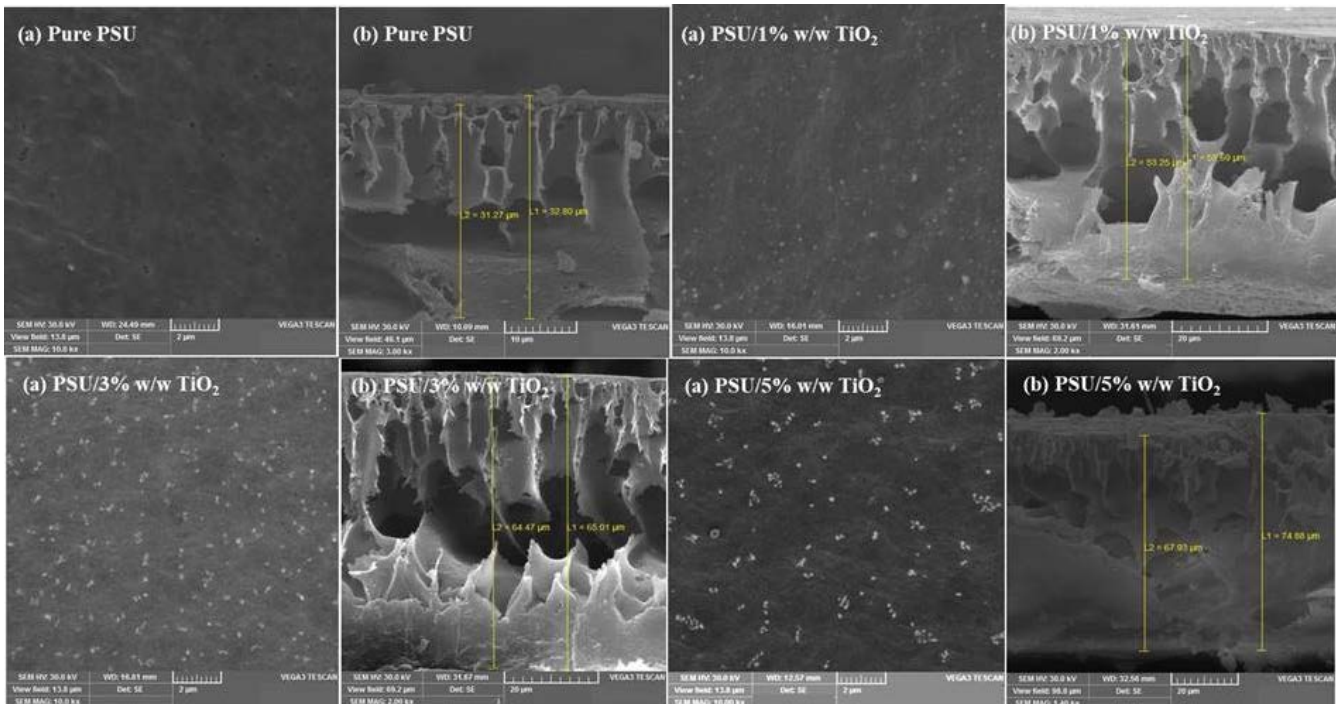
Fig. 6. Photomicrographs obtained by SEM of pure PSU membrane and hybrids with 1, 3, and 5% w/w TiO$_2$: (a) top surface and (b) cross-section.

due to the difference in chemical potential between the solvent (NMP) and the non-solvent (water). It begins in the region of the top surface of the membrane, the opposite region to that in contact with the glass substrate, and maintained throughout the section, however, with different intensities. In the photomicrographs obtained by SEM, asymmetric microporous membranes were observed with a selective layer (filtering skin) on top and a layer on the bottom with a variation in size and shape of pores along with its thickness [46]. It is from this difference in morphology in cross-section that arises the membrane's selectivity [47].

The pure PSU membrane (Fig. 6) presented a morphological structure with a regular slick layer and a small number of pores on its surface, for the studied increase. In addition, it is possible to observe a thinner cross-section (32.8 μm) followed by a fingers-shaped structure, macrovoids, microvoids, and the presence of agglomerates along its cross-section [48–51]. The addition of 1%, 3%, and 5% by weight of TiO$_2$ to the PSU membrane promoted the formation of a rough dense structure with the presence of agglomerates along with its surface layer [52–54]. In addition, the addition of TiO$_2$ nanoparticles promoted an increase in clusters size and in thickness of these hybrid membranes, with 1% (55.69 μm), 3% (65.01 μm), and 5% (74.88 μm) of TiO$_2$ when compared with the pure PSU membrane, which can be seen by its cross-sections, and this increase was directly proportional to the increase in the percentage of additive [24,27,29].

The addition of nanoparticles in polymeric membranes provides an increase in the number of pores on the top surface while the cross-section has become more crystalline and denser, being able to form rough aggregation on the top surface, due to the availability of electron pairs isolated from hydrogen atoms of polymer chain that can attract the inorganic charge. The increase in the concentration of nanoparticles for 5% w/w TiO$_2$ makes their distribution more uniform throughout their surface, also increasing the pore size due to rapid solidification of the membrane in the gelation bath. Furthermore, the support layer, which regulates the flow, became empty with the addition of load. This may be due to the demixing of polymer solution resulting from the nucleation and growth of the polymer-rich phase. This, in turn, regulated the rates of diffusion of coagulant and solvent through the skin layer, which led to the formation of macrovoids [25].

The addition of hydrophilic additives increases the viscosity of the polymeric solution. At low concentrations of additives, the hydrophilic effect of additives is dominant, which causes the formation of a nullified support layer similar to a more regular finger. However, in the high concentration of additives, the molten dope was less stable due to high viscosity. This dominant viscous effect delayed the rate of polymer demixing during membrane formation, resulting in a more spongy support layer [55].

TiO$_2$ has a specific surface area of 39.14 m^2 g^{-1}, an average particle diameter of 59.6 nm, a pores volume of 0.034 cm^3 g^{-1}, and an average pores diameter of 2.26 nm [56]. All these characteristics of inorganic material result in small nanometric particles with a porous structure that works favoring hydrophilicity, and the increase the permeate flow of hybrid membranes. The analysis of the structure of a membrane through the cross-section is as crucial as the top surface, considering that it is responsible for the

productivity of the membrane. Thus, it is essential that the membrane has good permeability and minimum resistance to the permeate flow at adequate pressures so that it can perform well.

3.5. Water vapor permeation

Fig. 7 illustrates the values obtained for the water vapor permeation of pure PSU membrane and hybrids with 1, 3, 5% w/w TiO_2.

In Fig. 7, pure PSU membrane presented the lower value of water vapor permeation (0.16×10^{-9} g Pa^{-1} s^{-1} m^{-1}), probably by obtaining a morphological structure containing superficial pores of smaller dimensions, presenting a smooth filter skin with few pores and low interconnectivity of these with the porous layer, as previously observed by SEM. The addition of TiO_2 to the PSU membrane promoted the formation of a rough dense structure with the presence of agglomerates along with its surface layer, and in addition, in general, it increased the fingers shaped structure, macrovoids, microvoids along its cross-section, increasing gradually the water vapor permeability for the membranes with 1% (0.18×10^{-9} g Pa^{-1} s^{-1} m^{-1}), 3% (0.21×10^{-9} g Pa^{-1} s^{-1} m^{-1}), and 5% (0.23×10^{-9} g Pa^{-1} s^{-1} m^{-1}) of TiO_2 additive when compared with the pure PSU membrane, and also as a result of the increase in the size and quantity of inorganic charge present on their top surfaces as observed previously by SEM images. In general, the introduction of hydrophilic inorganic fillers in the polymeric solution to obtain hybrid membranes results in an increase in water vapor permeation when compared with polymeric membranes without additives [57,58].

3.6. Contact angle

The interaction between the liquid and the solid makes the contact angle the most used method to measure the surface tension of solids. All membranes were evaluated with a drop of distilled water. The results obtained for the contact angles can be seen in Figs. 8 and 9.
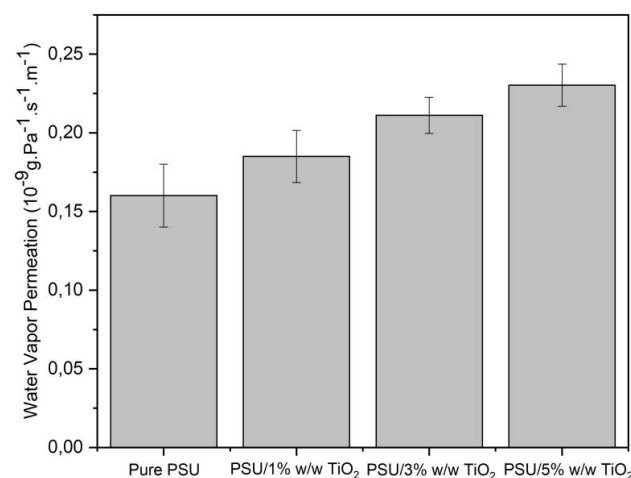
Analyzing Figs. 8 and 9, it appears that all membranes had a hydrophilic surface, considering that all angles are in range: $0° \leq \theta \leq 90°$. It was observed that pure PSU membrane showed had bigger contact angle, probably due to the existing porosity low in its surface layer, with a value of 71.88° initial time 10 s test, following certain stability over time, obtaining a value of 67.21° absorbing a small amount of water up to 300 s, in addition, this membrane had a smooth surface compared to other hybrid membranes [59].

The addition of TiO_2 provided lower contact angles compared to the pure PSU membrane, provided due to the formation of a morphological structure with a rough surface and the presence of agglomerates, in initial time 10 s test, with 1% (67.38°), 3% (63.64°), and 5% (60.79°) absorbing a small amount of water up to 300 s, with values of 65.39°, 60.80°, and 55.36°, respectively, result similar to what happened for the pure PSU membrane, as shown in Fig. 9. Furthermore, the bigger contact angles were obtained for the PSU membrane with 5% w/w TiO_2, due to the greater number of agglomerates present on the surface of this membrane [17,60]. The TiO_2 nanoparticles acted as porogenic agents and due to their hydrophilic character favored the absorption of water by the hybrid membranes. Furthermore, this increase in absorption was directly proportional to an increase in the percentage of TiO_2, resulting in lower values of contact angles.

3.7. Water and water/dye flux

The tests of measures of mass flow (J) of water were carried out at a pressure of 1.0 bar and temperature of 25°C. Fig. 10 show the flow measurement curves made with water for all membranes of pure PSU and their hybrids with 1, 3, and 5% w/w of TiO_2.

Hydraulic permeability is associated with the intrinsic characteristic of the membranes, due to the technique used in their preparation (phase inversion). In processes that use the pressure gradient as a driving force, the permeate flow is directly proportional to the pressure gradient

Fig. 7. Water vapor permeation of pure PSU membrane and hybrids with 1, 3, an 5% w/w TiO_2.
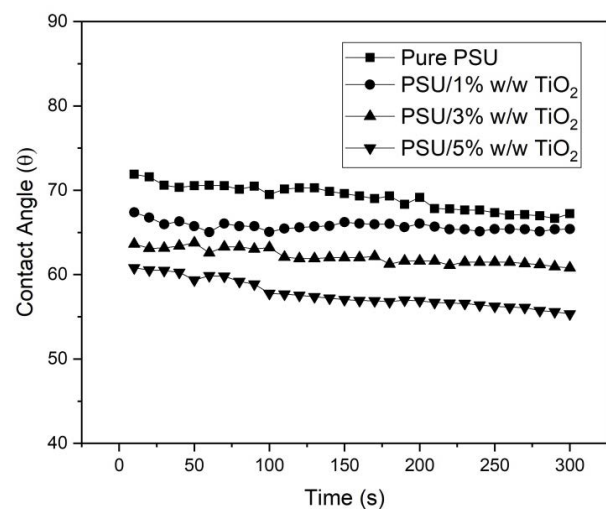
Fig. 8. Water contact angle of pure PSU membrane and hybrids with 1, 3, and 5% w/w TiO_2.
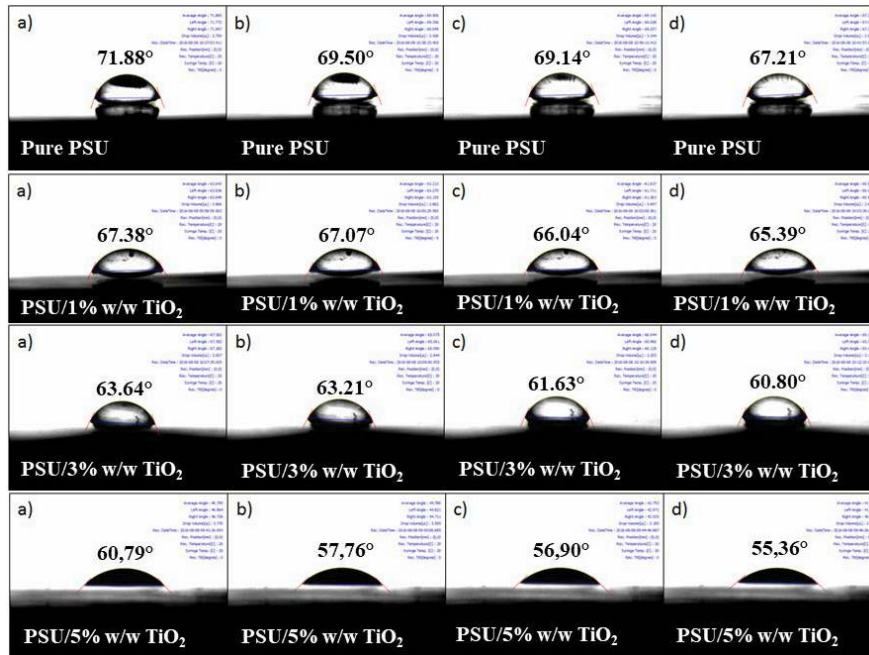
Fig. 9. Contact angles measurements of pure PSU membrane and hybrids with 1, 3, and 5% w/w TiO$_2$, at a time of (a) t = 10 s, (b) t = 100 s, (c) t = 200 s, and (d) t = 300 s.

itself, which is 1.0 bar. In these processes, the greatest contribution is related to the convective portion, representing the amount of solute that crosses the membrane (per unit area and time) due to the flow of the solvent itself, which is water.

From Fig. 10, it was initially possible to verify that the hybrid membranes with 1, 3, and 5% w/w of TiO$_2$ illustrated greater permeate flows for the water test, obtaining values of 2,163; 2,305; and 2,376 L h^{-1} m^{-2}, respectively, compared to the pure PSU that obtained an initial flow of 1,581 L h^{-1} m^{-2}, since the TiO$_2$ nanoparticles contributed to the formation of fingers, to having good interconnectivity with internal

pores present in cross-section, besides having a hydrophilic character [27,55,61–65].

Polysulfone membranes contain a sulfone group (O=S=O) in the main chain which is a polar group and provides hydrophilicity to the membrane, can be increased due to modification with the organic solvent (NMP) and the inorganic charge (TiO$_2$), mainly by the introduction of polar or charged functional groups. Furthermore, it was possible to notice that the flow measurements impregnated with water for all membranes decreased initially as mentioned previously and, shortly afterward, about 30 min later, there was some stability, possibly due to mechanical
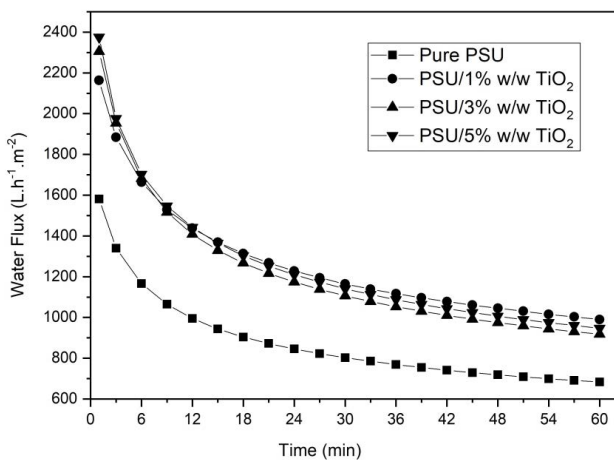
Fig. 10. Water flow curves for pure PSU membrane and its hybrids with 1, 3, and 5% w/w of TiO$_2$, at a pressure of 1.0 bar and temperature of 25°C.
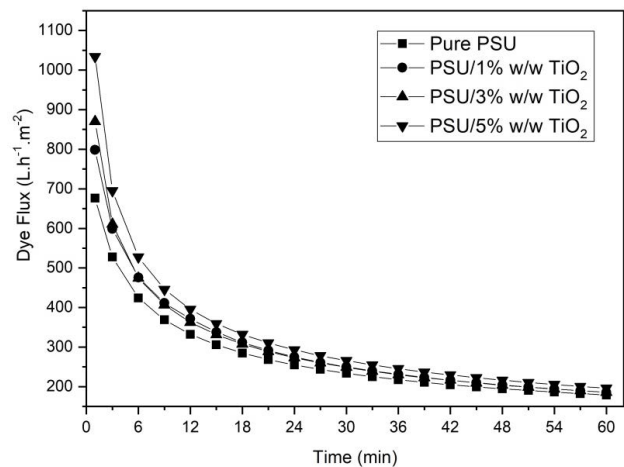
Fig. 11. Water/dye flow curves for pure PSU membrane and its hybrids with 1, 3, and 5% w/w of TiO$_2$, at pressures of 1.0 bar and temperature of 25°C.

compaction promoted by the applied pressure or possible swelling of the membranes [66–69]. This is because the polymer is hydrophilic and it was also verified in the contact angle that, over time, the membrane absorbs water and reduces the angle, also decreasing the flow obtained. Fig. 11 shows the flow curves made with water/dye for all membranes of pure PSU and their hybrids with 1, 3, and 5% w/w of TiO$_2$.

From Fig. 11, it was initially possible to verify that the hybrid membranes with 1, 3, and 5% w/w of TiO$_2$ illustrated greater permeate flows for the water/dye test, obtaining values of 800; 870; and 1,035 L h^{-1} m^{-2}, respectively, compared to the pure PSU that obtained an initial flow of 677 L h^{-1} m^{-2}, due to TiO$_2$ nanoparticles have a hydrophilic character facilitating the formation of fingers present in cross-section, as seen previously for the water permeate flow. One of the possible reasons for the declination of flow is increased dye concentration. As the membrane process proceeds, the concentration of dye tends to be greater than the feed concentration, which causes a layer of gel that causes the waterproofing and blocking of pores on the surface of membranes.

3.8. Spectrophotometry of ultraviolet-visible

Spectrophotometry of UV-vis is used for testing light absorption and light intensity on the properties of indigo blue dye what is a group of carbonyl compounds, one of the oldest dyes known in terms of natural dyes. In Fig. 12, we can observe the UV-vis spectroscopy of dye at a concentration of 500 mg L^{-1}. The visible light absorption area for indigo dye is at a wavelength of 600–900 nm (Fig. 12), with band maximum absorbance occurring at a wavelength of 720 nm, which is a characteristic value of indigo blue dye [70].

3.9. Dye retention

Fig. 13 shows the before and after treatment of water/dye effluents for the pure PSU membrane and its hybrids with 1, 3, and 5% w/w of TiO$_2$.

In Fig. 13, it is possible to observe the effluent before the treatment with the blue color and after separation by the membranes, the permeate was practically free of dye, showing the power of the membranes to remove and eliminate organic dye from solutions. Table 2 shows the indigo blue dye concentration in permeate (C_P), in feed (C_0), the rejection coefficient for the pure PSU membrane, and its hybrids with 1, 3, and 5% w/w of TiO$_2$.

The membranes tested in process of separating the indigo blue dye in water at a concentration of 500 mg L^{-1} (Table 2), achieved a significant reduction of dye in the permeate with rejection above 96%, and the highest rejection coefficient value was obtained for the hybrid membrane with 5% TiO$_2$, presenting 100% efficiency in colored contaminant separating. This high rejection may have contributed to the formation of a dye film with a concentration polarization close to the surface of these membranes, leading to fouling with blocked pores and hindering the passage of indigo blue dye [71,72]. Furthermore, these high rejections were due to the effects of combining size-exclusion along with electrostatic repulsion, which plays a critical role in dye separation for the membranes [73].

In general, dyes may form dimers in water, where trimers, tetramers, and other aggregates may form due
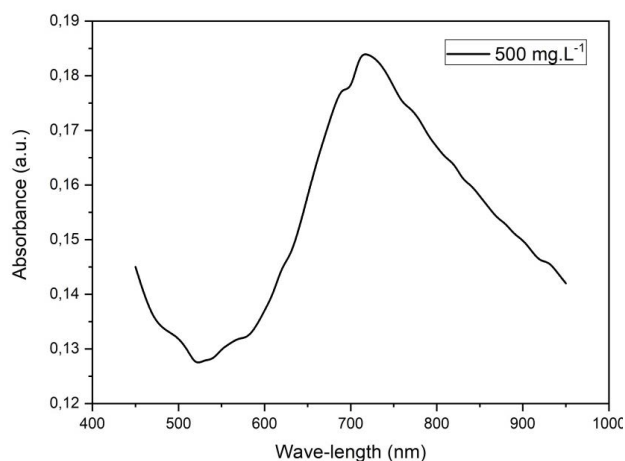
Fig. 12. Molecular absorption spectrum of indigo blue dye.

Table 2
Indigo blue dye concentration in feed suspension (C_0), in permeate (C_P), and the rejection coefficient for the membranes at a pressure of 1.0 bar using textile effluent

Membranes	C_0 (mg L^{-1})	C_P (mg L^{-1})	Rejection (%)
Pure PSU	500	19.2	96.2
PSU/1% w/w TiO$_2$	500	12.6	97.5
PSU/3% w/w TiO$_2$	500	6.7	98.7
PSU/5% w/w TiO$_2$	500	–	100.0
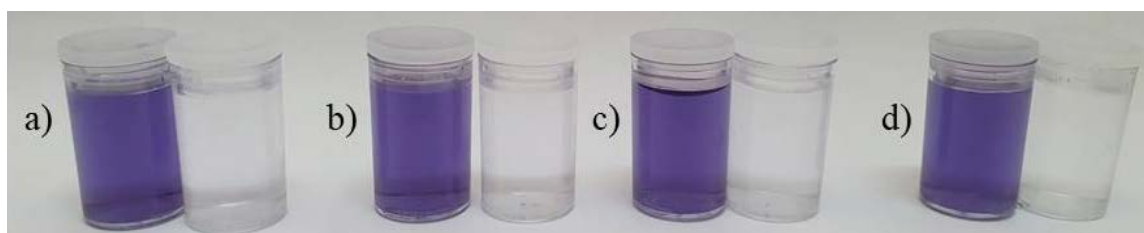
Fig. 13. Photos of before and after treatment of water/dye effluents by the membranes: (a) pure PSU, (b) 1% w/w, (c) 3 % w/w, and (d) 5% w/w of TiO$_2$.

to the agglomeration of dye dimers in a gradual manner, that association is caused by the amphiphilic nature of dye solutes and can be influenced by both structure and the different physical and chemical effects of dye [74]. The concentration polarization is inherent in any process of selective transport and establishes quickly on tangential type flows, contributing to the formation of a polarizing layer that provides additional resistance to mass transfer of solvent by the membrane, leading to a decrease in permeate flow and consequently increase in efficiency of dye separation.

4. Conclusions

Polysulfone flat membranes and hybrid with 1, 3, and 5% w/w titanium dioxide were successfully prepared. The introduction of TiO_2 to the polymeric solution was necessary to improve the hydrophilicity properties of polysulfone, also promoting rheological in solutions and morphological changes in obtained hybrid membranes. The pure PSU membrane showed less water vapor permeation of 0.16×10^{-9} g Pa^{-1} s^{-1} m^{-1} for having a hydrophobic character compared to membranes containing the inorganic component. The hybrid membranes showed contact angles less than 67.38° when compared to pure PSU membrane, due to the TiO_2 nanoparticles be hydrophilic and having acted as a porogenic agent. Excellent permeate flows were obtained in the tests carried out for water flux and effluent treatment at the pressure of 1.0 bar and temperature of 25°C, due to the existence of greater interconnectivity of the filtering skin with the porous layer and for the presence of the fingers existing along its cross-sections. The pollutant was treated by membranes through the size exclusion mechanism, separating, and retaining the dye molecules. Therefore, the water-dye separation tests of these membranes at a feed concentration of 500 mg L^{-1} with visible light absorption area for indigo dye with band maximum occurring in 720 nm, indicated a yield between 96% and 100%, presenting a great potential in microfiltration processes for textiles industry dyes separation.

References

[1] Z. Pan, C. Song, L. Li, H. Wang, Y. Pan, Y. Wang, X. Feng, Membrane technology coupled with electrochemical oxidation processes for organic wastewater treatment: recent advances and future prospects, Chem. Eng. J., 376 (2019) 120909 (1–19), doi: 10.1016/j.cej.2019.01.188.

[2] D.M. Warsinger, S. Chakraborty, E.W. Tow, M.H. Plumlee, C. Bellona, S. Loutatidou, L. Karimi, A.M. Mikelonis, A. Achilli, A. Ghassemi, L.P. Padhye, S.A. Snyder, S. Curcio, C.D. Vecitis, H.A. Arafat, J.H. Lienhard, A review of polymeric membranes and processes for potable water reuse, Prog. Polym. Sci., 81 (2018) 209–237.

[3] Q.C. Xia, M.L. Liu, X.L. Cao, Y. Wang, W. Xing, S.P. Sun, Structure design and applications of dual-layer polymeric membranes, J. Membr. Sci., 562 (2018) 85–111.

[4] P. Anadão, Membrane Science and Technology, Artliber Editora Ltda, São Paulo, 2010.

[5] K.C. Khulbe, C.Y. Feng, T. Matsuura, Synthetic Polymeric Membranes: Characterization by Atomic Force Microscopy, Springer-Verlag, Berlin, Heidelberg, 2008.

[6] A. Figoli, S. Simone, E. Drioli, Polymeric Membranes, N. Hilal, A.F. Ismail, C.J. Wright, Eds., Membrane Fabrication, CRC Press, Boca Raton FL, 2015.

[7] A. Kunz, S. Mukhtar, Hydrophobic membrane technology for ammonia extraction from wastewaters, Eng. Agric., 36 (2016) 377–386.

[8] R.W. Baker, Membrane Technology and Applications, John Wiley & Sons Inc., California, 2004.

[9] M. Mulder, Basic Principles of Membrane Technology, 2nd ed., Springer, Netherlands, 1996.

[10] J.M. Gohil, R.R. Choudhury, Introduction to nanostructured and nano-enhanced polymeric membranes: preparation, function, and application for water purification, Nanoscale Mater. Water Purif., (2019) 25–57, doi: 10.1016/B978-0-12-813926-4.00038-0.

[11] A. Kausar, Phase inversion technique-based polyamide films and their applications: a comprehensive review, Polym. Plast. Technol. Eng., 56 (2017) 1421–1437.

[12] M. Shaban, H. Abdallah, L. Said, H.S. Hamdy, K.A. Abdel, Titanium dioxide nanotubes embedded mixed matrix PES membranes characterization and membrane performance, Chem. Eng. Res. Des., 95 (2015) 307–316.

[13] M.S. Jyothi, V. Nayak, M. Padaki, R.G. Balakrishna, K. Soontarapa, Aminated polysulfone/TiO_2 composite membranes for an effective removal of Cr(VI), Chem. Eng. J., 283 (2016) 1494–1505.

[14] Y. Mansourpanah, S.S. Madaeni, A. Rahimpour, M. Adeli, M.Y. Hashemi, M.R. Moradian, Fabrication new PES-based mixed matrix nanocomposite membranes using poly-caprolactone modified carbon nanotubes as the additive: property changes and morphological studies, Desalination, 277 (2011) 171–177.

[15] C. Hoffmann, H. Silau, M. Pinelo, J.M. Woodley, A.E. Daugaard, Surface modification of polysulfone membranes applied for a membrane reactor with immobilized alcohol dehydrogenase, Mater. Today Commun., 14 (2018) 160–168.

[16] S.C. Mamah, P.S. Goh, A.F. Ismail, N.D. Suzaimi, L.T. Yogara-thinam, Y.O. Raji, T.H. El-Badawi, Recent development in modification of polysulfone membrane for water treatment application, J. Water Process Eng., 40 (2021) 101835 (1–20), doi: 10.1016/j.jwpe.2020.101835.

[17] P. Mobarakabad, A.R. Moghadassi, S.M. Hosseini, Fabrication and characterization of poly(phenylene ether-ether sulfone) based nanofiltration membranes modified by titanium dioxide nanoparticles for water desalination, Desalination, 365 (2015) 227–233.

[18] R. Mukherjee, S. De, Preparation of polysulfone titanium di oxide mixed matrix hollow fiber membrane and elimination of long term fouling by in situ photoexcitation during filtration of phenolic compounds, Chem. Eng. J., 302 (2016) 773–785.

[19] G.J. Summers, M.P. Ndawuni, C.A. Summers, Dipyridyl functionalized polysulfones for membrane production, J. Membr. Sci., 226 (2003) 21–33.

[20] N.A. Alenazi, M.A. Hussein, K.A. Alamry, A.M. Asiri, Modified polyether-sulfone membrane: a mini review, Des. Monomers Polym., 20 (2017) 532–546.

[21] S. Ioan, Functionalized Polysulfones: Synthesis, Charac-terization, and Applications, Taylor & Francis Group, LLC, CRC Press, Boca Raton FL, 2015.

[22] N.K.O. Cruz, G.U. Semblante, D.B. Senoro, S. You, S. Lu, Dye degradation and antifouling properties of polyvinylidene fluoride/titanium oxide membrane prepared by sol–gel method, J. Taiwan Inst. Chem. Eng., 45 (2014) 192–201.

[23] G. Ghasemzadeh, M. Momenpour, F. Omidi, M.R. Hosseini, M. Ahani, A. Barzegari, Applications of nanomaterials in water treatment and environmental remediation, Front. Environ. Sci. Eng., 8 (2014) 471–482.

[24] M.R. Esfahani, J.L. Tyler, H.A. Stretz, M.J. Wells, Effects of a dual nanofiller, nano-TiO_2 and MWCNT, for polysulfone-based nanocomposite membranes for water purification, Desalination, 372 (2015) 47–56.

[25] R. Krishnamoorthy, V. Sagadevan, Polyethylene glycol and iron oxide nanoparticles blended polyethersulfone ultrafiltration membrane for enhanced performance in dye removal studies, E-Polymers, 15 (2015) 151–159.

[26] C. Evangeline, V. Pragasam, K. Rambabu, S. Velu, P. Monash, G. Arthanareeswaran, F. Banat, Iron oxide modified

polyethersulfone/cellulose acetate blend membrane for enhanced defluoridation application, Desal. Water Treat., 156 (2019) 177–188.

[27] Y. Yang, H. Zhang, P. Wang, Q. Zheng, J. Li, The influence of nano-sized TiO_2 fillers on the morphologies and properties of PSU UF membrane, J. Membr. Sci., 288 (2007) 231–238.

[28] M. Baghbanzadeh, D. Rana, C.Q. Lana, T. Matsuura, Effects of inorganic nano-additives on properties and performance of polymeric membranes in water treatment, Sep. Purif. Rev., 45 (2016) 141–167.

[29] N.A.A. Hamid, A.F. Ismail, T. Matsuura, A.W. Zularisam, W.J. Lau, E. Yuliwati, M.S. Abdullah, Morphological and separation performance study of polysulfone/titanium dioxide (PSF/TiO_2) ultrafiltration membranes for humic acid removal, Desalination, 27 (2011) 85–92.

[30] N.A.L. Flower, K.M. Rahulan, R.A. Sujatha, R.A. Sharath, J. Darson, C. Gopalakrishnan, Fabrication of silver nano-particles decorated polysulfone composite membranes for sulfate rejection, Appl. Surf. Sci., 493 (2019) 645–656.

[31] ASTM, ASTM E 96/E 96M-05, Standard Test Methods for Water Vapor Transmission of Materials, Philadelphia, 2005.

[32] S. Velu, K. Rambabu, P. Monash, C. Sharma, Improved hydrophilic property of PES/PEG/$MnCO_3$ blended membranes for synthetic dye separation, Int. J. Environ. Stud., 75 (2018) 592–604.

[33] S.M. Torres, C.M. Esteves, J.L. Figueiredo, A.M. Silva, Thin-film composite forward osmosis membranes based on polysulfone supports blended with nanostructured carbon materials, J. Membr. Sci., 520 (2016) 326–336.

[34] T.D. Kusworo, N. Ariyanti, D.P. Utomo, Effect of nano-TiO_2 loading in polysulfone membranes on the removal of pollutant following natural-rubber wastewater treatment, J. Water Process Eng., 35 (2020) 101190 (1–11), doi: 10.1016/j.jwpe.2020.101190.

[35] A. Matioli, J. Miagava, D. Gouvêa, Modification of stability of polymorphs of nanometric TiO_2 by excess SnO_2 surface, Ceramica, 58 (2012) 53–57.

[36] J.M. Yeh, C.L. Chen, Y.C. Chen, C.Y. Ma, H.Y. Huang, Y.H. Yu, Enhanced corrosion prevention effect of polysulfone-clay nanocomposite materials prepared by solution dispersion, J. Appl. Polym. Sci., 92 (2004) 631–637.

[37] X. Wei, Z. Wang, J. Wang, S.A. Wang, A novel method of surface modification to polysulfone ultrafiltration membrane by preadsorption of citric acid or sodium bisulfite, Membr. Water Treat., 3 (2012) 35–49.

[38] A. Mushtaq, H.B. Mukhtar, A.M. Shariff, FTIR study of enhanced polymeric blend membrane with amines, Res. J. Appl. Sci. Eng. Technol., 7 (2014) 1811–1820.

[39] A.T. Kuvarega, N. Khumalo, D. Dlamini, B.B. Mamba, Polysulfone/N, Pd co-doped TiO_2 composite membranes for photocatalytic dye degradation, Sep. Purif. Technol., 191 (2018) 122–133.

[40] M.Y. Naz, S. Ahmad, S. Shukrullah, N. Altaf, A. Ghaffar, Effect of microwave plasma treatment on membrane structure of polysulfone fabricated using phase inversion method, Mater. Today: Proc., (2020) 1–4 (in Press), doi: 10.1016/j.matpr.2020.04.522.

[41] S. Yu, J. Zhu, J. Liao, H. Ruan, A. Sotto, J. Shen, Homogeneous trimethylamine-quaternized polysulfone-based anion exchange membranes with crosslinked structure for electrodialysis desalination, Sep. Purif. Technol., 257 (2020) 117874 (1–10), doi: 10.1016/j.seppur.2020.117874.

[42] H. Jiang, T. Wang, S. Li, Z.P. Zhao, Fabrication of porous polymer membrane from polysulfone grafted with acid ionic liquid and the catalytic property for inulin hydrolysis, J. Membr. Sci., 618 (2021) 118742 (1–15), doi: 10.1016/j.memsci.2020.118742.

[43] H.M. Mousa, H. Alfadhel, M. Ateia, A.A. Gomaa, G.T.A. Jaber, Polysulfone-iron acetate/polyamide nanocomposite membrane for oil-water separation, Environ. Nanotechnol. Monit. Manage., (2020) 100314 (1–9), doi: 10.1016/j.enmm.2020.100314.

[44] S. Mondal, S.K. Majumder, Fabrication of the polysulfone-based composite ultrafiltration membranes for the adsorptive removal of heavy metal ions from their contaminated aqueous

solutions, Chem. Eng. J., 401 (2020) 126036 (1–18), doi: 10.1016/j.cej.2020.126036.

[45] A.A. Bernardes, M.C.S. Bulhosa, F.F. Gonçalves, M.G. D'oca, S.I. Wolke, J.H.Z. Santos, Materiais SiO_2-TiO_2 for photocatalytic degradation of diuron, New Chem., 34 (2011) 1343–1348.

[46] A. Sarihan, E. Eren, B. Eren, Y. Erdoğan, Flux-enhanced polysulfone membranes blended with ABPBI as a novel additive, Mater. Today Commun., 20 (2019) 100594 (1–6), doi: 10.1016/j.mtcomm.2019.100594.

[47] K.M. Medeiros, V.N. Medeiros, D.F. Lima, C.A.P. Lima, E.M. Araújo, H.L. Lira, Hybrid microporous membranes applied in wastewater treatment, Macromol. Symp., 383 (2019) 1800037 (1–7), doi: 10.1002/masy.201800037.

[48] L.G.M. Baldo, M.K. Lenzi, D. Eiras, Water vapor permeation and morphology of polysulfone membranes prepared by phase inversion, Polym. Sci. Technol., 30 (2020) e2020027 (1–8), doi: 10.1590/0104-1428.05820.

[49] F.H. Azhar, Z. Harun, K.N. Yusof, S.S. Alias, N. Hashim, E.S. Sazali, A study of different concentrations of bio-silver nanoparticles in polysulfone mixed matrix membranes in water separation performance, J. Water Process Eng., 38 (2020) 101575 (1–10), doi: 10.1016/j.jwpe.2020.101575.

[50] Y.X. Xie, K.K. Wang, W.H. Yu, M.B. Cui, Y.J. Shen, X.Y. Wang, B.K. Zhu, Improved permeability and antifouling properties of polyvinyl chloride ultrafiltration membrane via blending sulfonated polysulfone, J. Colloid Interface Sci., 579 (2020) 562–572.

[51] M. Nadoura, F. Boukraa, A. Ouradia, A. Benaboura, Effects of methylcellulose on the properties and morphology of polysulfone membranes prepared by phase inversion, Mater. Res., 20 (2017) 339–348.

[52] V. Vatanpour, H. Rabiee, M.H.D.A. Farahania, M.M. Fara-hanid, M. Niakan, Preparation and characterization of novel nanoporous SBA-16-COOH embedded polysulfone ultrafiltration membrane for protein separation, Chem. Eng. Res. Des., 156 (2020) 240–250.

[53] Y. Zhang, F. Liu, Y. Lu, L. Zhao, L. Song, Investigation of phosphorylated TiO_2–SiO_2 particles/polysulfone composite membrane for wastewater treatment, Desalination, 324 (2013) 18–126.

[54] M.S. Fahmey, A.H.M. El-Aassar, M.M.A. Elfadel, A.S. Orabi, R. Das, Comparative performance evaluations of nanomaterials mixed polysulfone: a scale-up approach through vacuum enhanced direct contact membrane distillation for water desalination, Desalination, 451 (2019) 111–116.

[55] K. Rambabu, S. Velu, Improved performance of $CaCl_2$ incorporated polyethersulfone ultrafiltration membranes, Period. Polytech., Chem. Eng., 60 (2016) 181–191.

[56] S.A. Pascoal, C.B. Silva, K.S. Silva, G.G.C. Lima, K.M. Medeiros, C.A.P. Lima, Treatment by TiO_2/UV of wastewater generated in polymeric membranes production, Desal. Water Treat., 207 (2020) 30–42.

[57] E.A. Santos Filho, A.F. Salviano, B.A. Araújo, K.M. Medeiros, V.N. Medeiros, E.M. Araújo, H.L. Lira, Influence of additives on hybrids membranes morphology for water treatment, Diffus. Found., 14 (2017) 86–106.

[58] M.M.C.C. Mota, E.M. Araújo, A.M.D. Leite, K.M. Medeiros, C.A.P. Lima, PA6/sodium clay membrane for application in petroleum sector, Mater. Sci. Forum, 930 (2018) 264–269.

[59] E.A. Santos Filho, K.M. Medeiros, E.M. Araújo, R.S.B. Ferreira, S.S.L. Oliveira, V.N. Medeiros, Membranes of polyamide 6/clay/salt for water/oil separation, Mater. Res. Express, 6 (2019) 105313 (1–13), doi: 10.1088/2053-1591/ab3754.

[60] Z. Zhao, K. Muylaert, A. Szymczyk, I.F.J. Vankelecom, Harvesting microalgal biomass using negatively charged polysulfone patterned membranes: influence of pattern shapes and mechanism of fouling mitigation, Water Res., 188 (2021) 116530 (1–11), doi: 10.1016/j.watres.2020.116530.

[61] A. Modi, J. Bellare, Efficiently improved oil/water separation using high flux and superior antifouling polysulfone hollow fiber membranes modified with functionalized carbon nanotubes/graphene oxide nanohybrid, J. Environ. Chem. Eng., 7 (2019) 102944 (1–9), doi: 10.1016/j.jece.2019.102944.

[62] J.F. Li, Z.L. Xu, H. Yang, L.Y. Yu, M. Liu, Effect of TiO_2 nanoparticles on the surface morphology and performance of microporous PES membrane, Appl. Surf. Sci., 255 (2009) 4725–4732.

[63] A. Razmjoua, J. Mansouri, V. Chena, The effects of mechanical and chemical modification of TiO_2 nanoparticles on the surface chemistry, structure and fouling performance of PES ultrafiltration membranes, J. Membr. Sci., 378 (2011) 73–84.

[64] D. Emadzadeh, W.J. Lau, T. Matsuura, M.R. Sisakht, A.F. Ismail, A novel thin film composite forward osmosis membrane prepared from $PSf-TiO_2$ nanocomposite substrate for water desalination, Chem. Eng. J., 237 (2014) 70–80.

[65] R. Kumar, A.M. Isloor, A.F. Ismail, S.A. Rashid, A.A. Ahmed, Permeation, antifouling and desalination performance of TiO_2 nanotube incorporated PSf/CS blend membranes, Desalination, 316 (2013) 76–84.

[66] L. Zhu, M. Wu, B.V.D. Bruggen, L. Lei, Zhu L, Effect of TiO_2 content on the properties of polysulfone nanofiltration membranes modified with a layer of TiO_2-graphene oxide, Sep. Purif. Technol., 242 (2020) 116770 (1–12), doi: 10.1016/j.seppur.2020.116770.

[67] Y. Zhang, X. Shan, Z. Jin, Y. Wang, Synthesis of sulfated Y-doped zirconia particles and effect on properties of polysulfone membranes for treatment of wastewater containing oil, J. Hazard. Mater., 192 (2011) 559–567.

[68] A. Tizchang, Y. Jafarzadeh, R. Yegani, S. Khakpour, The effects of pristine and silanized nanodiamond on the performance of polysulfone membranes for wastewater treatment by MBR system, J. Environ. Chem. Eng., 7 (2019) 103447 (1–10), doi: 10.1016/j.jece.2019.103447.

[69] K. Tempelman, S. Casanova, N.E. Benes, The effect of hydrocarbon pollution on polysulfone-based membranes in aqueous separations, Sep. Purif. Technol., 224 (2019) 348–355.

[70] A. Bouzidi, I.S. Yahia, M.S.A. El-Sadek, Novel and highly stable indigo (C.I. Vat Blue I) organic semiconductor dye: crystal structure, optically diffused reflectance and the electrical conductivity/dielectric behavior, Dyes Pigm., 146 (2017) 66–72.

[71] R.S.B. Ferreira, A.F. Salviano, S.S.L. Oliveira, E.M. Araújo, V.N. Medeiros, H.L. Lira, Treatment of effluents from the textile industry through polyethersulfone membranes, Water, 11 (2019) 2540 (1–11), doi: 10.3390/w11122540.

[72] R.C.O. Lima, H.L. Lira, G.A. Neves; M.C. Silva, K.B. França, Use of ceramic membrane for indigo separation in effluent from textile industry, Mater. Sci. Forum, 789 (2014) 537–541.

[73] K. Rambabu, G. Bharath, P. Monash, S. Velu, F. Banat, M. Naushad, G. Arthanareeswaran, P.L. Show Effective treatment of dye polluted wastewater using nanoporous $CaCl_2$ modified polyethersulfone membrane, Process Saf. Environ., 124 (2019) 266–278.

[74] J. Gao, Z. Thong, K.Y. Wang, T.S. Chung, Fabrication of loose inner-selective polyethersulfone (PES) hollow fibers by one-step spinning process for nanofiltration (NF) of textile dyes, J. Membr. Sci., 541 (2017) 413–424.